Rizzolio et al.

Neuropilin-1 upregulation elicits adaptive resistance to oncogene-targeted therapies

SUPPLEMENTAL FIGURES

Suppl. Fig. 1

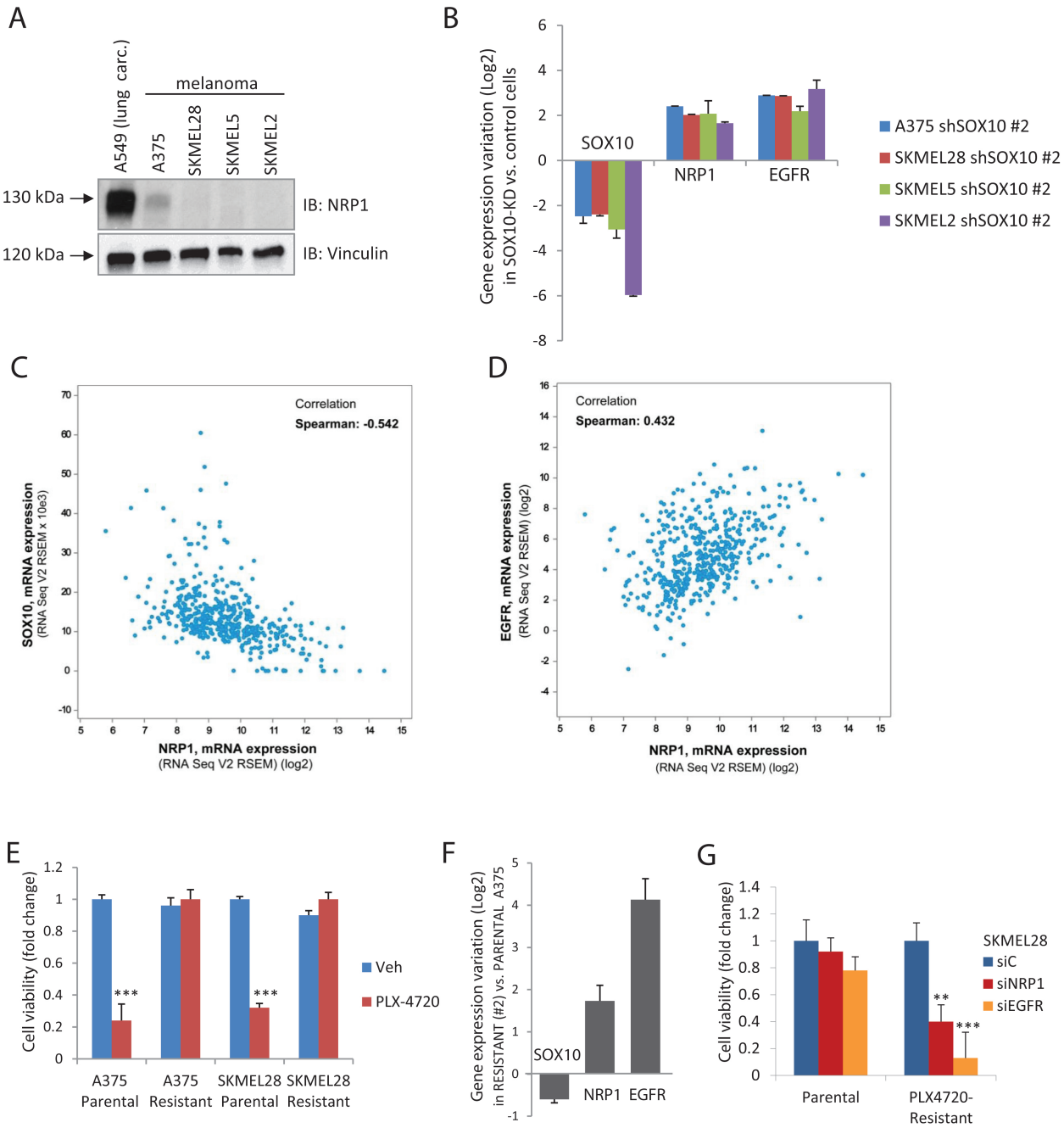

Suppl. Figure 1.

A. Western blotting analysis of NRP1 expression in A549 lung carcinoma cells and in a panel of different melanoma cells; vinculin provided whole protein loading control (n=3). **B.** A375, SK-MEL-28, SK-MEL-5 (BRAF mutated) and SK-MEL-2 (BRAF wild type) melanoma cells were subjected to SOX10 knock-down by an shRNA (#2, independent from that applied for data shown in Fig. 1A), and mRNA expression of *SOX10*, *NRP1* and *EGFR* was analyzed by quantitative Real-Time PCR. Plotted in the graph are fold-change variations (Log2 scale) measured in SOX10-depleted cells vs. respective controls (n=5). **C.** Dot plot representing inverse correlation between *SOX10* and *NRP1* mRNA expression, based on analysis of the TCGA provisional melanoma dataset (n= 469 melanoma samples). **D.** Dot plot representing direct correlation between *NRP1* and *EGFR* mRNA expression, based on analysis of the TCGA provisional melanoma dataset (n= 469). **E.** The viability of A375 and SKMEL28 Parental (BRAF inhibitor sensitive) and targeted therapy-Resistant cells was assessed (by Cell Titer Glo Viability Assay) in the presence (or absence) of 2 μM PLX-4720 BRAF inhibitor (n>3). **F.** mRNA expression of *SOX10*, *NRP1* and *EGFR* (analyzed by quantitative Real-Time PCR) in another batch of A375 cells (beyond that shown in main Fig. 1C) which stably developed acquired resistance to 2 μM PLX-4720 (n=3). Plotted in the graph are fold-change variations (Log2 scale) measured in drug-Resistant vs. Parental cells. **G.** The viability of SKMEL28 cells, Parental or Resistant to PLX-4720, was assessed upon *NRP1* or *EGFR* knock-down with targeted siRNAs (n=4). Statistical significance was calculated vs. respective cells treated with control siRNAs (siC); Bonferroni correction was applied for multiple sample comparisons.

Suppl. Fig. 2

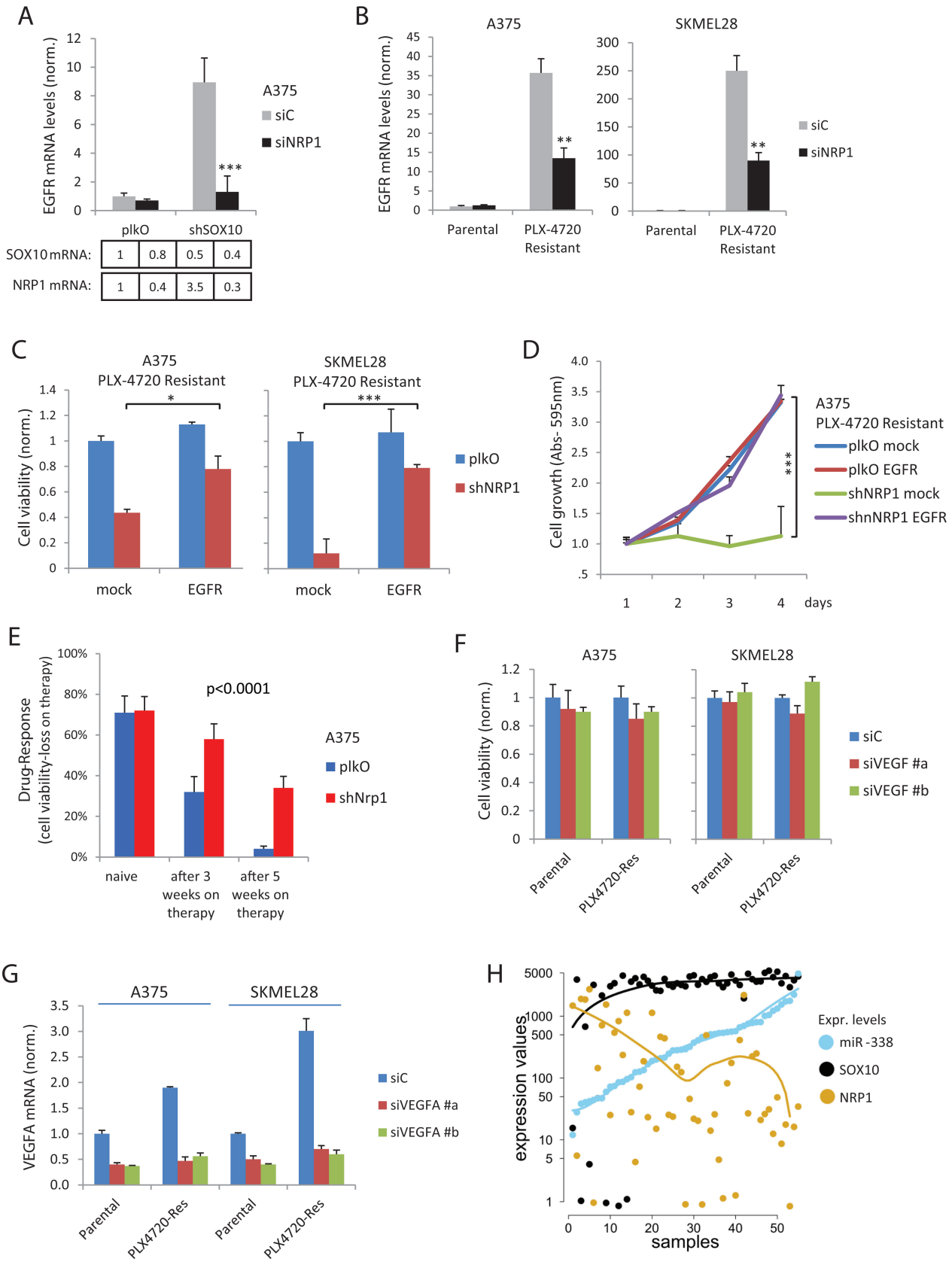
A
EGFR mRNA levels (norm.)
A375
siC
siNRP1
***
plkO
shSOX10
SOX10 mRNA:
1
0.8
0.5
0.4
NRP1 mRNA:
1
0.4
3.5
0.3
B
A375
SKMEL28
EGFR mRNA levels (norm.)
**
Parental
PLX-4720 Resistant
siC
siNRP1
C
A375
PLX-4720 Resistant
SKMEL28
PLX-4720 Resistant
Cell viability (norm.)
mock
EGFR
plkO
shNRP1
D
Cell growth (Abs- 595nm)
A375
PLX-4720 Resistant
plkO mock
plkO EGFR
shNRP1 mock
shnNRP1 EGFR
days
E
Drug-Response
(cell viability-loss on therapy)
p<0.0001
A375
plkO
shNrp1
naive
after 3 weeks on therapy
after 5 weeks on therapy
F
A375
SKMEL28
Cell viability (norm.)
siC
siVEGF #a
siVEGF #b
Parental
PLX4720-Res
G
A375
SKMEL28
VEGFA mRNA (norm.)
siC
siVEGFA #a
siVEGFA #b
Parental
PLX4720-Res
H
expression values
samples
Expr. levels
miR -338
SOX10
NRP1

Suppl. Figure 2.

A. qPCR analysis of EGFR expression in control or SOX10-depleted A375 cells, subjected to NRP1 knock-down (validated by qPCR analysis; normalized values shown at the bottom) (n=4). **B.** Similar to the previous panel, EGFR mRNA expression was analyzed by qPCR in Parental or PLX-4720-Resistant A375 cells (left graph) or SKMEL28 melanoma cells (right graph), upon NRP1 silencing (validated by qPCR: over 70% knock-down) (n=4). Plotted values are normalized to Parental controls (siC). **C.** PLX4720-Resistant cells, A375 (left graph) or SKMEL28 (right graph), subjected (or not) to NRP1 silencing to restore drug-sensitivity, were furthermore transfected to overexpress EGFR (or mock), and cell viability in presence of the BRAF-inhibitor was assessed in the different conditions (n>3). Statistical significance was calculated comparing EGFR transfected cells vs. respective mock controls. **D.** EGFR-mediated recovery of cell viability assessed in PLX4720-Resistant cells as growth curve (n>3). The analysis of statistical significance (with Bonferroni-corrected two-ways Anova) compared EGFR transfected cells vs. respective mock controls. **E.** The fraction of control or NRP1-depleted A375 cells sensitive to 0.5 μM PLX-4720 was inferred, based on residual cell viability, either in naïve parental cells or in cells subjected to the drug for three or five weeks (instigating resistance onset). Two-ways Anova test (Bonferroni-corrected) was applied to compare NRP1-KD samples with respective controls (n>3). **F-G.** Parental or PLX4720-resistant melanoma cells (A375 on the left and SKMEL28 on the right) were subjected to VEGFA silencing by means of two independent siRNAs (#a and #b). (F) Cell viability was assessed (by means of Cell Titer Glo Viability Assay) at 72h from reverse transfection (n=3). (G) *VEGF* mRNA silencing was validated by qPCR analysis, in the same cells analyzed in panel F (n=3). **H.** Scatter dot plot representing the expression profiles of miR-338-3p (Blue), *SOX10* (Black), and *NRP1* (Gold) in a panel of 57 different melanoma cells, available at Geo Dataset Series GSE89438 (Andrews et al., 2016). The dots (samples) were ordered on X axis according to miR-338 levels. Y axis (Log scale) indicates expression values (TPM for miRNA, normalized expression values for coding genes). A fit-curve for each gene was calculated with LOESS function in R. Correlation Spearman values for SOX10/miR-338 = 0.539 (p= 2.92E-05); for miR-338/NRP1 = -0.391 (p= 0.003); for SOX10/NRP1 = -0.359 (p= 0.007).

Cited Reference: *Andrews MC, Cursons J, Hurley DG, Anaka M, Cebon JS, Behren A, Crampin EJ. Systems analysis identifies miR-29b regulation of invasiveness in melanoma. Mol Cancer. 15:72 (2016).*

Suppl. Fig. 3

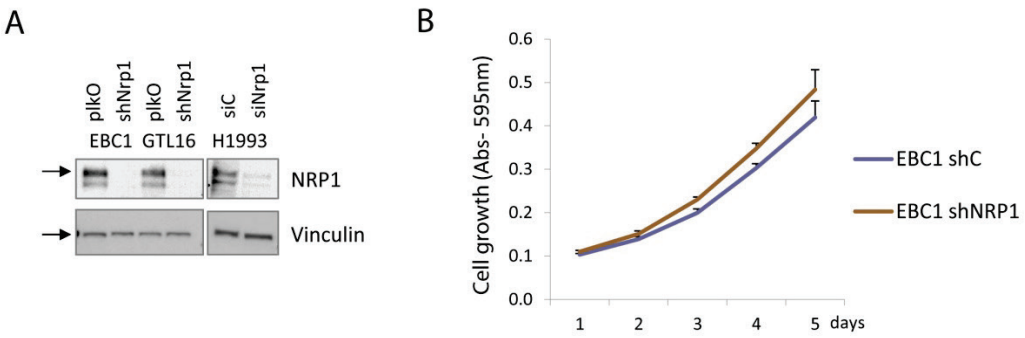

Suppl. Figure 3.

A. Western blotting analysis demonstrates NRP1 expression knock-down with shRNAs in three different Met-addicted cell lines; vinculin provided a protein loading control (n>3). **B.** Analysis of EBC1 cell growth upon NRP1 silencing (or control), scored by crystal violet cell staining at different time points (n>3).

Suppl. Fig. 4

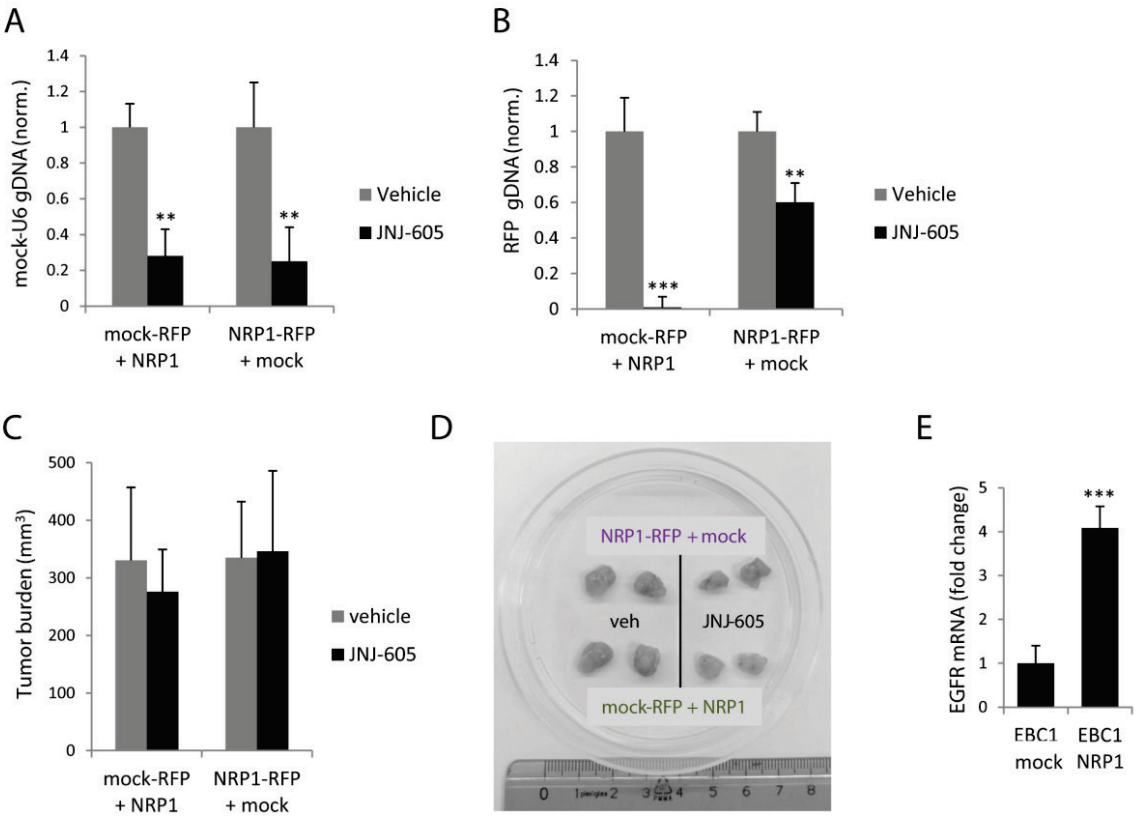

Suppl. Figure 4.

A. The presence of mock-transduced cells in the heterogeneous tumors shown in Fig. 4C was scored at the end of the experiment by measuring with qPCR in the genomic DNA of explanted xenografts the relative representation of the U6 genetic marker present in the control vector plkO. In the graph are plotted fold-change variations of mock cells content, observed in tumors treated with JNJ-605 vs. untreated tumors (n=5, per each experimental condition). **B.** The presence of RFP-labelled cells in the tumors shown in Fig. 4C was scored at the end of the experiment by measuring by qPCR the relative representation of the RFP genetic marker in the genomic DNA of explanted xenografts. The graph shows fold-change variations of RFP-labeled cells content, in treated vs. untreated heterogeneous tumors, either containing mock-RFP or NRP1-RFP cells (n=5, per each experimental condition). **C.** The volume of tumor xenografts, in the different experimental conditions shown in Fig. 4C and in the above panels, was scored by external measurement at the end of the experiment (n=5, per each experimental condition). **D.** Representative images of heterogeneous tumors described in Fig. 4C (and panel C in this figure), after explant at the end of the experiment. **E.** EGFR mRNA levels were measured by quantitative Real-Time PCR in EBC1 cells, either control (plkO) or overexpressing NRP1 (n=3).

Suppl. Fig. 5

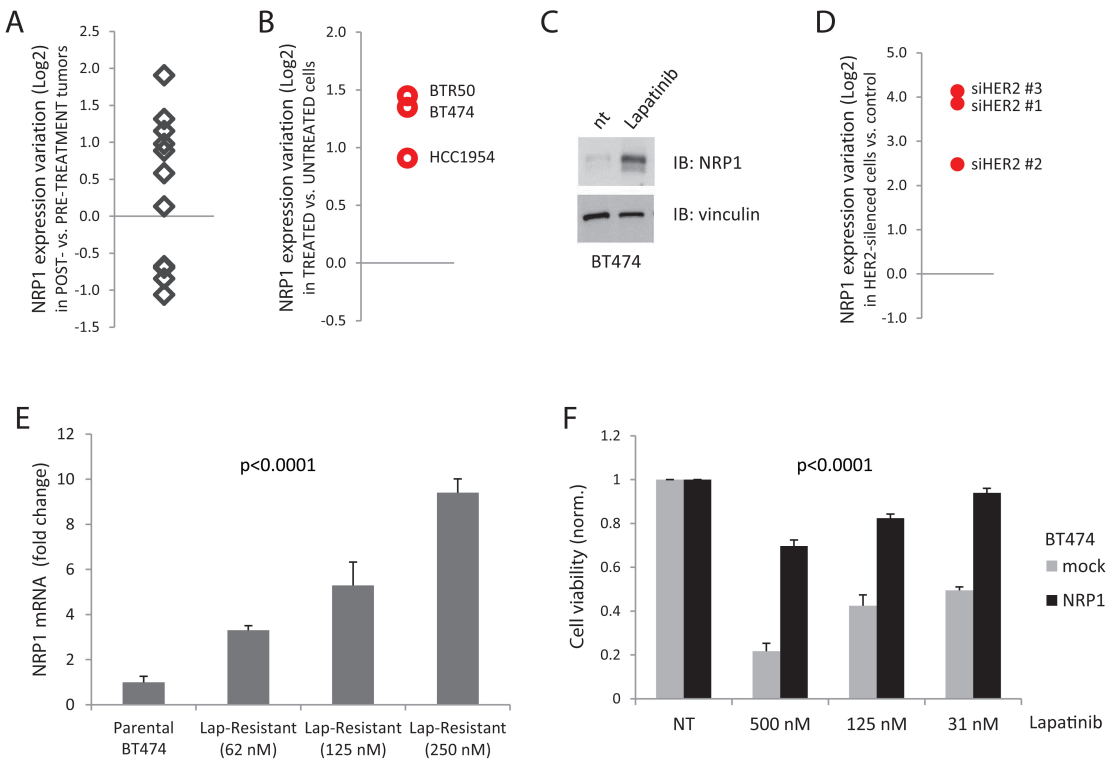

Suppl. Figure 5.

A. The graph shows *NRP1* expression variations in a panel of 11 paired breast cancer samples taken from the same patients before and on treatment with HER2 inhibitors (RNAseq values plotted as Log2 ratio of treated/untreated; see Methods for further details). **B.** *NRP1* expression variations in three indicated breast cancer cell lines treated with the HER2 inhibitor trastuzumab (analysis of RNAseq dataset published in (Merry et al., 2015); values plotted as Log2 ratio of treated/untreated). **C.** Immunoblotting analysis of NRP1 expression in BT4T4 cells treated with the HER2-inhibitor lapatinib (250 nM for 24 hours) (n=4). **D.** *NRP1* expression variations in BT474 cells elicited by HER2 knock-down by three independent siRNAs (analysis of RNAseq dataset published in (Merry et al., 2015); values plotted as Log2 ratio of siRNA treated/control) (n>3). **E.** NRP1 mRNA expression levels were measured, by quantitative Real-Time PCR, in BT474 cells which acquired resistance to the indicated increasing concentrations of the HER2 inhibitor lapatinib ("Lap-Resistant" cells) (n>3). **F.** Cell viability of BT474, either NRP1-overexpressing or mock-transfected, kept in the presence of the indicated concentrations of lapatinib for 72 hours (n>3). Statistical significance was calculated comparing NRP1-overexpressing cells and mock controls, in each treatment condition. Statistical analysis was done by Bonferroni-corrected Anova tests.

Cited Reference: *Merry, C. R., McMahon, S., Thompson, C. L., Miskimen, K. L., Harris, L. N., and Khalil, A. M.. Integrative transcriptome-wide analyses reveal critical HER2-regulated mRNAs and lincRNAs in HER2+ breast cancer. Breast Cancer Res Treat 150, 321-334 (2015).*

Suppl. Fig. 6

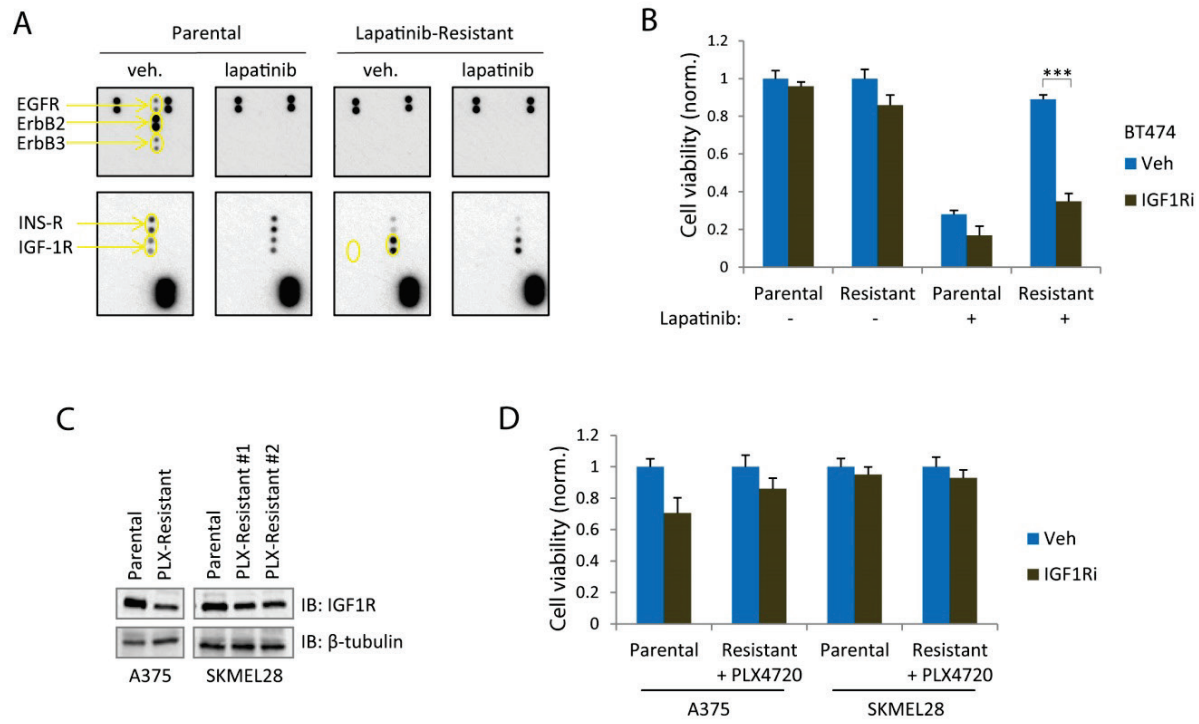

Suppl. Figure 6.

A. A phospho-protein antibody-capture array, detecting 42 different tyrosine kinase receptors (Proteome Profiler Array, R&D Systems), was hybridized with protein cell lysates derived from either parental or lapatinib-resistant BT474 cells (in presence or absence of the drug, 250nM, for 24 hours). Arrows indicate the dots corresponding to capturing antibodies specifically detecting the indicated tyrosine phosphorylated kinases. Other positive signals are represented by reference positive controls for array orientation. Upper row images were taken after short membrane exposure, while lower row images show the sole additional positive dots revealed by long membrane exposure. **B.** Cell viability of Parental or Lapatinib-Resistant BT474 cells, subjected to single or combination treatments with 250 nM Lapatinib and/or the IGF1R inhibitor BMS-754807 (IGF1Ri, 25 nM) (n>5). The statistical significance was calculated comparing cells with and without IGF1R-inhibitor in the different conditions (applying Bonferroni correction). **C.** Immunoblotting analysis of IGF1R expression in parental or PLX4720-Resistant melanoma cells A375 and SKMEL28; β-tubulin provided a loading control (representative experiment, of three repetitions). **D.** The viability of parental or PLX4720-Resistant melanoma cells A375 and SKMEL28 was assessed, upon treatment with 100 nM IGF1R inhibitor BMS-754807 (n>3).

Suppl. Fig. 7

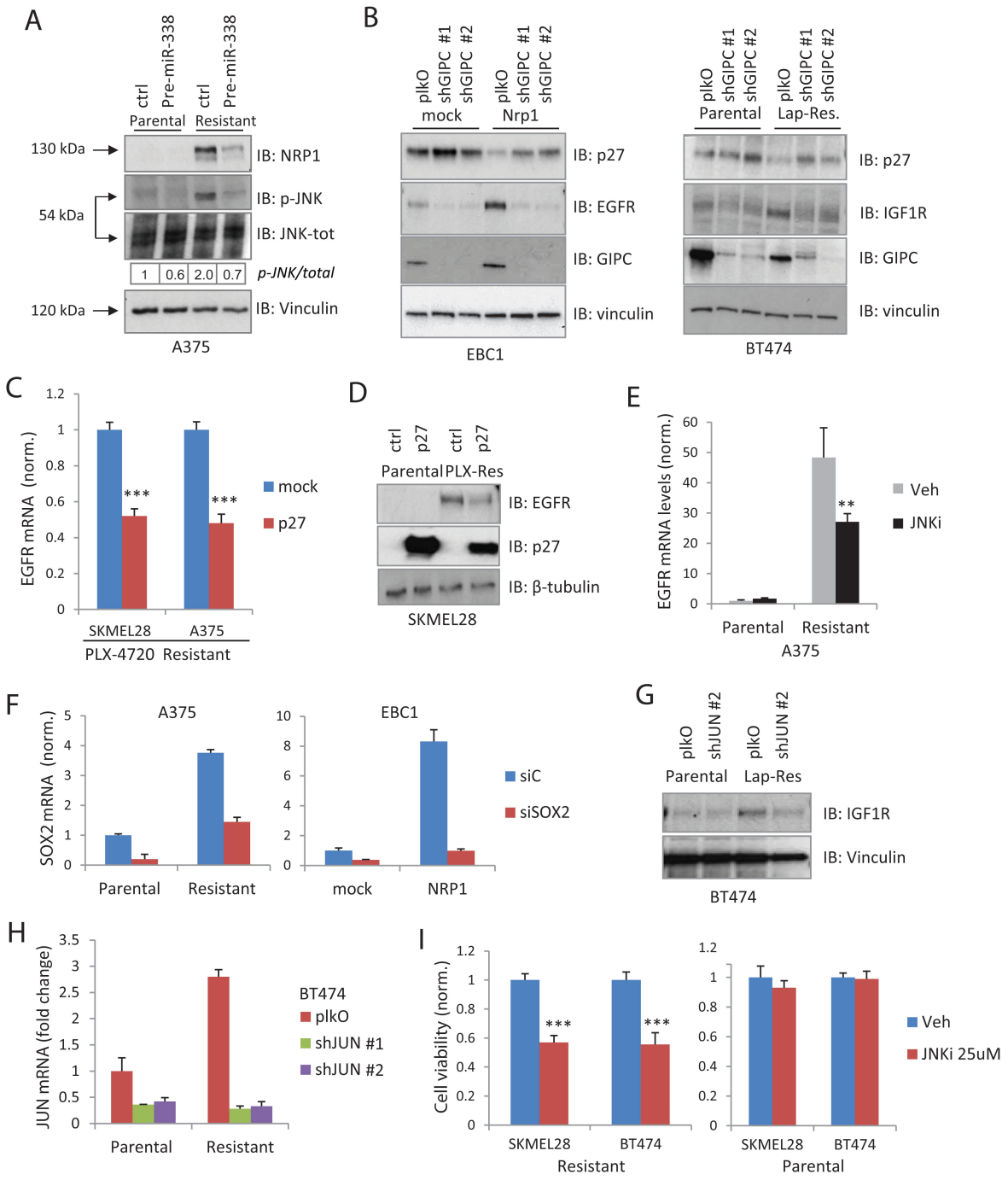

Suppl. Figure 7.

A. Immunoblotting analysis of NRP1 and pJNK levels in parental or PLX-4720-resistant A375 melanoma cells, upon forced miR-338 expression (by pre-miRNA transfection); duplicate samples were run on parallel gels and vinculin provided a loading control (n=3). The values at the bottom indicate densitometric measurement of relative p-JNK vs. total JNK band intensity. **B.** Immunoblotting analysis revealed that GIPC silencing by shRNAs in NRP1-overexpressing EBC1 (left) and BT474 drug resistant cells (right) impacts on p27, EGFR and IGF1R expression; vinculin provided the loading control (n=4). **C-D.** p27 overexpression in drug-resistant melanoma cells A375 and SKMEL28 leads to EGFR downregulation (detected by qPCR

analysis and immunoblotting; duplicate samples were run on parallel gels)(n=3). **E.** qPCR analysis of EGFR expression in drug-resistant A375 cells treated with 25 µM JNK-inhibitor SP600125 (n=3). **F.** qPCR analysis validating SOX2 knock-down in control and NRP1-overexpressing EBC1 cells (analyzed in main Fig. 7J). **G.** Immunoblotting analysis of IGF1R expression in Parental or Lapatinib-Resistant BT474 cells, subjected to JUN silencing with an alternative shRNA construct, compared to that applied in main Fig. 8E. **H.** *JUN* knock-down by two independent shRNAs (applied in experiments in Fig. 8E and Suppl. Fig. 7G) was validated by qPCR. **I.** Cell viability was assessed upon JNK inhibition in: NRP1-dependent PLX-4720-Resistant SKMEL28, or Lapatinib-Resistant BT474 cells (in presence of the relative drugs), and in the respective parental cells (n>3). The statistical significance, in each condition, was calculated comparing JNKi-treated vs. untreated cells.

Suppl. Fig. 8

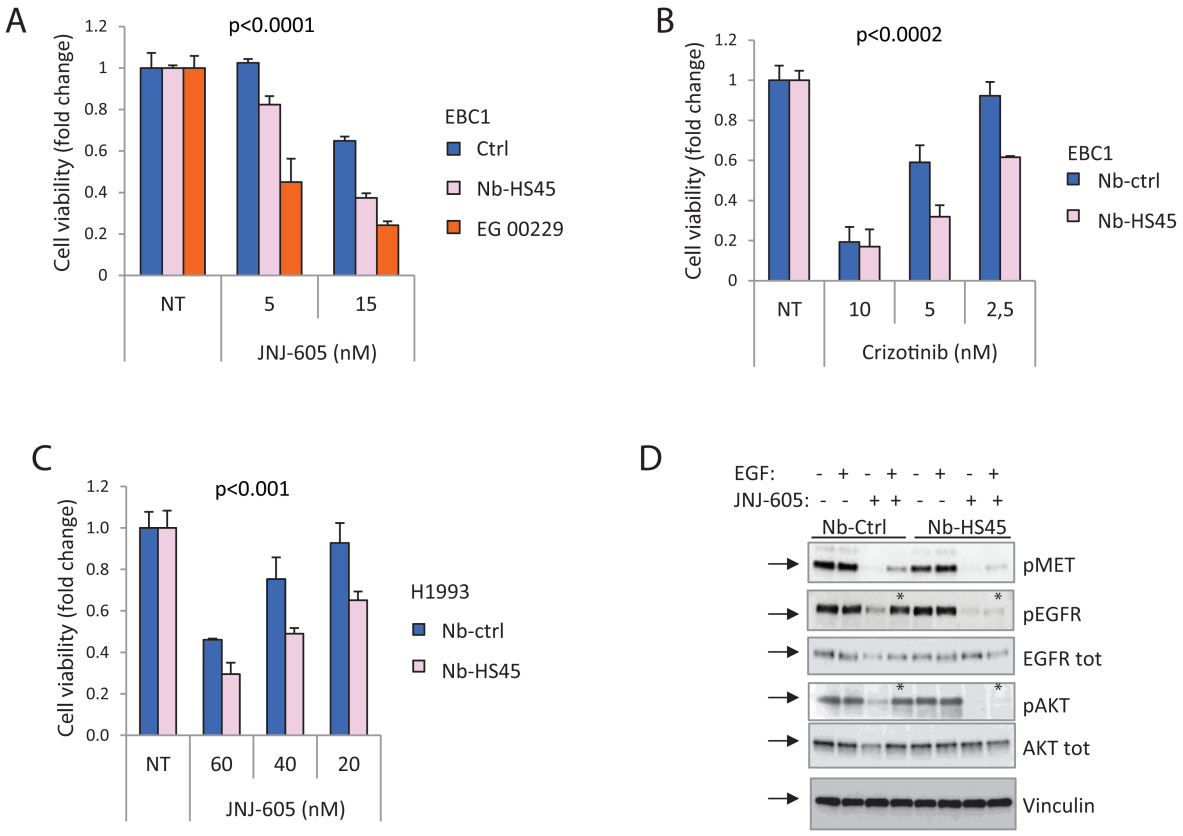

Suppl. Figure 8.

A. The bar graph shows the viability (assessed by Cell Titer Glo) of EBC1 cells treated with the indicated concentrations of the Met-inhibitor JNJ-605, alone, or in combination with either the NRP1-targeted small molecule EG00229 (12.5 μM) or the NRP1-binding nanobody HS45 (5 μg/ml) (n>3). **B.** The viability of EBC-1 cells was assessed upon treatment with the indicated concentrations of the TKI crizotinib, either alone or in combination with the NRP1-targeted nanobody HS45 (5 μg/ml)(n>3). **C.** The viability of H1993 Met-addicted cells was assessed upon treatment with the indicated concentrations of the Met kinase inhibitor JNJ-605, either alone or in combination with the NRP1-targeted nanobody HS45 (5 μg/ml)(n>3). **D.** Western blot analysis of EBC1 cells upon treatment with the Met-inhibitor JNJ-605 (40 nM), in presence or absence of EGF (1 ng/ml), either or not in association with the NRP1-targeted nanobody HS45 (5 μg/ml) (n=3; duplicate samples were run on parallel gels for staining with different antibodies). Data show the expression and the phosphorylation levels of EGFR, as well as of its intracellular effector AKT; vinculin provided whole protein loading control. In all panels, the statistical analysis was done by two-ways Anova tests, with Bonferroni correction.

Suppl. Fig. 9

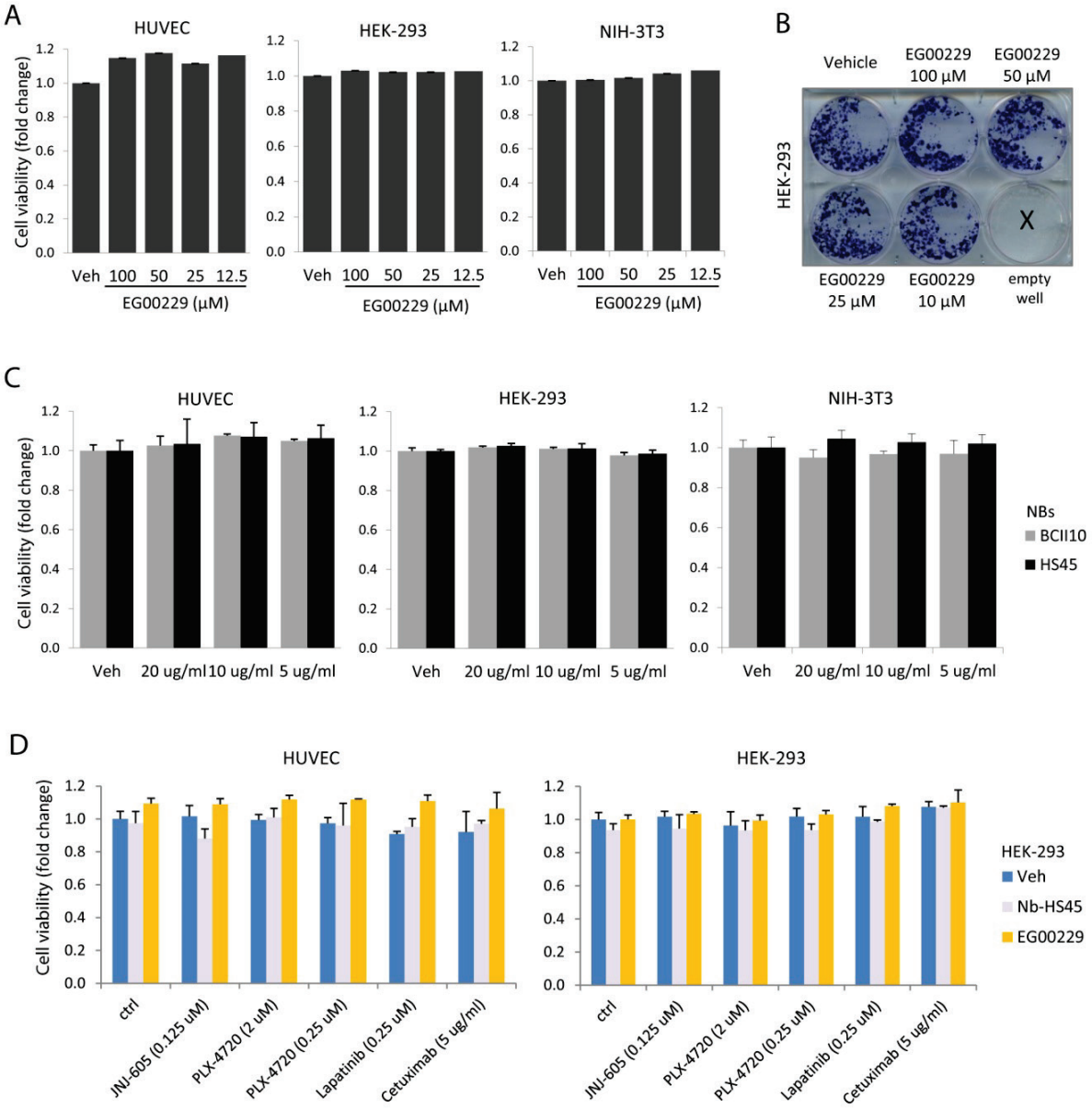

Suppl. Figure 9.

A. The viability of diverse non-tumoral cells (HUVEC, HEK-293 and NIH-3T3) was assessed after 72 hours in presence of the indicated concentrations of NRP1-targeted drug EG00229 (up to 8-fold higher that those applied to tumor cells in main Fig. 8), or vehicle alone (n>3). **B.** Long-term, two-week growth assay of HEK-293 cells (initial seeding 5000 cells/well) in presence of the indicated concentrations of EG00229. The image shows cells grown in 5 differently treated wells, fixed and stained with crystal-violet at the end of the experiment. **C.** The viability of diverse non-tumoral cells (as in panel A) was assessed after 72 hours in presence of the indicated concentrations of NRP1-targeted nanobodies HS45 or non-targeted control NBs BCII10 (up to 4-fold higher than those applied to tumor cells in Fig. 8) (n>3). **D.** Combined treatments of normal HUVEC endothelial and HEK-293 kidney cells with high doses of NRP1-targeted molecules (20 μg/ml HS45 nanobodies, 100 μM EG00229) or vehicle alone, in association with the indicated concentrations of oncogene-targeted drugs (n>3).